*DOI:*
10.1161/CIRCEP.117.005107

*Document Version*
Peer reviewed version

# ST elevation magnitude correlates with right ventricular outflow tract conduction delay in Type I Brugada ECG

Kevin MW Leong* MRCP[1,2]; Fu Siong Ng* MRCP PhD[1,2]; Cheng Yao PhD[3]; Caroline Roney PhD[1]; Patricia Taraborrelli PhD[2]; Nicholas WF Linton MRCP PhD; Zachary I Whinnett MRCP PhD[1,2]; David C Lefroy FRCP FHRS[2]; D Wyn Davies MD FRCP FHRS[2]; Phang Boon Lim MRCP PhD[1,2]; Sian E Harding PhD FESC[1]; Nicholas S Peters MD FRCP FHRS[1,2]; Prapa Kanagaratnam PhD FRCP[1,2]; Amanda M Varnava MD FRCP[2]

*joint first authors

**[1]National Heart & Lung Institute, Imperial College London, UK**

**[2]Imperial College Healthcare NHS Trust, London, UK**

**[3]Medtronic Ltd, UK**

**Running title:** *ST elevation in BrS correlates to conduction delay*

**Address for correspondence:**

Dr Amanda Varnava

Consultant Cardiologist

Imperial College Healthcare NHS Trust

Hammersmith Hospital

London, W12 0HS

Tel: 020 33131000

Email: avarnava@doctors.org.uk

**Manuscript word count: 5748 words**

**Journal Subject Terms: Electrophysiology, Pathophysiology, Mechanisms**

## Abstract

**Introduction**

The substrate location and underlying electrophysiological mechanisms that contribute to the characteristic ECG pattern of Brugada Syndrome (BrS) are still debated. Using non-invasive electrocardiographical imaging (ECGi), we studied whole heart conduction and repolarization patterns during ajmaline challenge in BrS individuals.

**Methods and Results**

13 participants (mean age 44±12 yrs; 8 males), 11 concealed Type I BrS patients and 2 healthy controls, underwent an Ajmaline infusion with ECGI and ECG recordings. ECGi activation recovery intervals (ARI) and activation timings across the right ventricle (RV) body, outflow tract (RVOT), and left ventricle (LV) were calculated and analysed at baseline and when Type I BrS pattern manifested following ajmaline. Peak J-ST point elevation was calculated from the surface ECG, and compared to the ECGi derived parameters at the same time point.

Following ajmaline infusion, the RVOT had the greatest increase in conduction delay (5.4±2.8ms vs 2.0±2.8ms vs 1.1±1.6ms; *p=0.007*) and ARI prolongation (69±32ms vs 39±29ms vs 21±12ms; *p=0.0005*) compared to RV or LV. In controls, there was minimal change in J-ST point elevation, conduction delay or ARI at all sites with ajmaline. In BrS patients, conduction delay in RVOT, but not RV or LV, correlated to the degree of J-ST point elevation (Pearson R 0.81, $p<0.001$). No correlation was found between J-ST point elevation and ARI prolongation in the RVOT, RV or LV.

**Conclusion**

Magnitude of ST (J point) elevation in the Type I BrS pattern is attributed to degree of conduction delay in the RVOT and not prolongation in repolarization time.

**Key words:** Brugada Syndrome, Non-invasive Electrocardiographical Imaging (ECGi), Repolarisation, Depolarisation, Sodium Channel Blockade

## Introduction

Both abnormalities in repolarization and depolarization have been described in BrS, although which of these mechanisms give rise to the ST segment elevation (STE) in the Type I pattern remain unclear[1]. The varying degree of STE observed within different BrS subjects likely reflects different degrees of conduction and/or repolarization heterogeneity in the epicardial right ventricular outflow tract (RVOT), as suggested by previous clinical studies[2-4].

Body surface mapping potential and echocardiographic surrogates of conduction over the RV, but not repolarization, have been found to correlate with STE following sodium channel blockade in BrS[2,3]. In contrast, single contact electrode data from electrophysiological catheters situated in the epicardial and endocardial RVOT demonstrated that STE corresponded to prolongation of repolarization in the epicardial RVOT following pilsicainide[4]. Currently, high density, epicardial data characterising the relationship of STE to changes in conduction and repolarization is lacking.

Electrocardiographical imaging (ECGi) is a novel tool that utilises body surface potentials from a 252-electrode vest, and using inverse solution mathematics, reconstructs >1200 unipolar electrograms onto a digitised epicardial heart surface. It is possible to observe patterns of depolarization and repolarization using this method and it has also been used to study the electrophysiological substrate in a variety of conditions[5,6].

In this study, we aimed to characterise whole heart electrophysiological conduction and repolarization patterns on the epicardial surfaces of BrS hearts following ajmaline infusion. We also correlated these changes to the degree of J point elevation of the ST segment on the surface ECG to further elucidate the mechanisms that underlie the Type I ECG in BrS.

## Methods

### *Subject enrolment*

Patients referred to our centre for an Ajmaline challenge for suspected Brugada Syndrome were recruited. Individuals were referred for the test as part of a family screen or based on clinical history and ECG findings. All patients were required to withhold all concurrent medications 5 days before the test.

### *Study protocol*

ECGi (EcVUE system, Medtronic) and 15 lead surface ECG recordings were simultaneously performed at resting baseline and throughout the ajmaline challenge. The ECGi methodology has been described and validated previously[7]. Briefly, body surface potential data obtained via a 252-electrode vest was combined with patient specific heart-torso geometry derived from a thoracic CT scan. Using inverse solution mathematical algorithms, the ECGi system reconstructed epicardial unipolar electrograms (EGM) and panoramic activation maps over a single sinus beat which was visualised on a digitised image of the patient's heart **(Figure 1a)**.

A total ajmaline dose of 1mg/kg was administered and infused over a period of 5 minutes. The infusion was prematurely stopped in the event of manifestation of the Type 1 BrS pattern or prolongation of the QRS interval by 130%. Recordings were discontinued once the 15 lead ECG had returned to baseline, or for a period of at least 20 minutes where no ECG changes were observed. The study protocol was reviewed and approved by our institutional review committee (ref:14/LO/1318). All subjects gave informed consent.

***Changes in activation time duration from ECGi***

3-D activation maps were automatically generated from the ECGi system and are based on local activation timings (LAT), defined as the steepest negative deflection (-dV/dt) during the QRS complex, of the unipolar EGM. Activation maps were generated at baseline and following ajmaline (at manifestation of BrS pattern in responders or end of infusion in non-responders) and the activation timing window of interest were synchronised to allow comparison across phases. Activation maps over three consecutive beats were checked at each phase to ensure consistency. Analysis and detection of differences in activation patterns across the phases was carried out by two of the reviewers and where interpretation differed a third reviewer arbitrated. A surrogate for right ventricular outflow tract (RVOT), right ventricular (RV) and left ventricular (LV) free walls activation time duration (ATD) was derived from the difference in EGM local activation time between two points, 3.5 centimetres apart, in the direction of the activation wavefront within their respective regions pre-ajmaline. This was compared to the RVOT, RV and LV ATD derived from the same locations post ajmaline. Anatomical landmarks on CT scan were used to define the regions: - i) left anterior descending artery separated the RV and LV, ii) the outflow tract was defined as the region within the RV 4cm below the pulmonary valve. An example of ATD measurement in the RVOT is shown in **Figure 2**.

***Activation recovery intervals from ECGi unipolar EGMs***

For each patient, the left and right ventricles were anatomically divided into 15 regions **(Figure 1b),** from which 45 unipolar EGMs (3 per region) were analysed during a cardiac cycle at each of the following phases: - i) pre-ajmaline ii) post-ajmaline. EGM analysis was performed using an off-line semi-automated custom-made programme with Matlab (Mathworks Inc, USA). Activation recovery interval (ARI), a surrogate of action potential (AP)

duration or index of myocardial repolarization time, was taken from the LAT to the steepest negative deflection (-dV/dt) of a positive T wave, or the steepest positive deflection (+dV/dt) of a negative or biphasic T wave of the unipolar EGM **(Figure 1b)**[8]**.** As ARI vary with heart rate, values were corrected using the Bazett's formula (ARIc). Changes in both ARI and ARIc in the RVOT, RV and LV following ajmaline were subsequently computed. Changes in RVOT transepicardial ARI/ARIc dispersion were also calculated which was defined as the maximum difference between ARI/ARIc values within this region. A detailed ARI map of the RVOT region was also derived to illustrate the changes in response to ajmaline in one patient. As such an electroanatomical map could not be automatically produced by the EcVUE version of the ECGi system, ARI was individually derived from over 100 points within the RVOT region before and after ajmaline. Contour maps were subsequently created using a graphical software package (Surfer 13, Golden Software LLC, Colorado) with the data obtained.

***15 lead surface ECG analysis***

Tpeak-end duration (Tped) reflects transmural dispersion of repolarization and was calculated in the precordial leads as shown in **figure 1c** using digital calipers by a reviewer blinded to patient details[9]. Manifestation of the Type I BrS pattern (J point elevation ≥2mm within the coved ST segment and negative T wave in ≥1 precordial RV lead) was confirmed by 2 study investigators on the 15 lead ECG[10]. The J point was defined as the junction between the end of the QRS complex and the beginning of the ST-segment[11]. J point elevation was the distance in millimetres from the isoelectric baseline determined with digital calipers (**figure 1c**). The ST segment at 40ms ($ST_{40}$) and 80ms ($ST_{80}$) from this point was also obtained. The time point at which the diagnostic BrS pattern became evident on the 15 lead ECG was noted and simultaneously corroborated on the ECGi system. Changes in conduction (ATD) and

repolarization (ARI/ARIc) derived from the ECGi system were studied between the two phases: i) pre-ajmaline and ii) post-ajmaline – at the point when Type I BrS pattern manifest. In cases where the ajmaline challenge yielded a negative result, the post-ajmaline phase was taken at the 6 minute point following commencement of the infusion. For each patient, the maximal J point and ST (J-ST) elevation from the precordial leads was calculated from the surface ECG using digital calipers. Maximal J-ST point elevation was correlated with the amount of change in ATD, ARI/ARIc and Tped in each region. Changes in Tped within RV/RVOT region is represented by the lead with maximal J-ST point elevation within V1 and V2 in the $2^{nd}$, $3^{rd}$ and $4^{th}$ intercostal spaces, and lead V5 for the LV. As transepicardial dispersion of repolarization also exists in the BrS phenotype, J-ST point elevation was also correlated with the change in RVOT ARI/ARIc transepicardial dispersion.

***Statistical Analysis***

Changes in ATD, ARI/ARIc and Tped from baseline were calculated for the RVOT, RV and LV in each individual, with pooled mean change and standard deviation presented for each anatomical region. Difference between the three regions in mean change in ATD and ARI/ARIc following ajmaline were compared using a one-way ANOVA. The Newman-Keuls multiple comparison test was utilized in the post-hoc analysis if ANOVA was significant. Where a two -group comparison of continuous variables was appropriate, the unpaired t-test was employed. Correlation was calculated using Pearson's correlation coefficient. Statistical analysis was performed using GraphPad PRISM v5 (Graphpad Software Inc, USA), and a p value of $<0.05$ was considered significant.

**Results**

***Patient characteristics***

Thirteen patients underwent Ajmaline challenge with ECGi and 15 lead surface ECG recordings (mean age 44±12 years; 8 males). Eleven of these had a Type I BrS pattern induced on the surface ECG. A positive diagnosis was reached between 1.5 to 6 minutes of the ajmaline infusion. Manifestation of the Type I pattern occurred within leads V1 and V2 in the $2^{nd}$, $3^{rd}$ and $4^{th}$ intercostal spaces. No ventricular arrhythmias were induced during the infusion. **Table 1** summarises the clinical characteristics of all participants. Two patients (12 and 13) had BrS excluded following a negative Ajmaline challenge and served as controls in the study.

***Effect of Ajmaline on whole heart activation pattern***

A representative example of 3D activation map before and after ajmaline in a BrS patient is shown (**Figure 2a**). Conduction slowing within the RVOT, as evidenced by greater amount of isochronal crowding or increase in ATD between two fixed points, can be observed after the appearance of the Type I BrS pattern following ajmaline. In all 11 BrS patients, an increase in ATD was preferentially seen in the RVOT compared to the RV and LV (5.4±2.8ms vs 2.0±2.8ms vs 1.1±1.6ms; *ANOVA p=0.0007*) (**Figure 2b**). In contrast, no significant differences were observed between the RVOT, RV and LV in the controls (2.1±0.1ms vs 1.5±0.7ms vs 1.0±1.4ms; *ANOVA p=0.58*).

***Effect of Ajmaline on EGM morphology and whole heart repolarization***

Alterations in EGM morphology were observed in BrS patient and not in controls. Representative examples of EGMs are shown before and after ajmaline in a BrS and control patient (**Figures 3a i and ii**). Manifestation of coved ST segment elevation along with negative

T wave could be observed in EGMs restricted to the RVOT region (**Figure 3ai**), although no such changes were observed in the control patient (**Figure 3aii**). ARI was observed to preferentially prolong in the RVOT region in comparison to the RV and LV (39±32ms vs 12±30ms vs 2±19ms; *ANOVA p=0.0056*) (**Figure 3b**). A similar picture was observed with ARIc (69±32ms vs 39±29ms vs 21±12ms; *ANOVA p=0.0005*). In the controls, no differences in ARI/ARIc prolongation between regions were observable (*ANOVA p=0.50 and p=0.45 respectively*).

The mean increase in Tped was similarly larger in leads over the RVOT/RV than LV in the BrS group (19±7 vs 1±2; *p=0.004*) (**Table 2**). Prolongation in Tped in the RV lead, where maximal ST elevation was observed, was larger than the LV lead (V5) (21±18ms vs 2±13ms, *p=0.013*). No significant difference was observed between the RV/RVOT and LV for controls following ajmaline (2±3ms vs 1±0.5ms, *p=0.512*)

***Correlation of ATD, ARI/ARIc and Tpeak-end duration with J-ST point elevation***

To investigate the effect changes in conduction and repolarization within the epicardial RVOT have on J point elevation following ajmaline, we correlated change in ATD and ARI/ARIc with maximal J point elevation. A strong correlation was observed between increase in ATD in the RVOT and J point elevation (Pearson R=0.81, *p=0.0009*) (**Figure 4a**) but not in the RV (R=0.27, *p=0.*36) and LV (R=0.21, *p=0.49*), where a 1mm increase in J point elevation equated to an increase in ATD by 1.44±0.32ms in the RVOT. In addition, there was no significant correlation between ARI/ARIc prolongation and J point elevation in any region (ARI - RVOT: R=0.33, *p=0.27*; RV: R=-0.08, *p=0.79*; LV: R=-0.07, *p=0.82*) (ARIc - RVOT: R=0.51, *p=0.07*; RV: R=0.13, *p=0.66*; LV: R=0.40, *p=0.18*) (**Figure 4b**). J point elevation was also not observed to correlate with Tped changes in any of the RV/RVOT and LV leads (**Table 2**). No significant correlation to

J elevation was also observed when compared to Tped changes in the RV lead where maximal J elevation was observed (**Figure 4c**).

Transepicardial heterogeneity of the AP duration, or dispersion of ARI/ARIc, may exist within the RVOT in BrS. At baseline, there was a higher but non-significant difference in ARI dispersion in BrS patients when the BrS ECG was not manifest (35±27ms vs 13±5; *p=0.3*). Following ajmaline, ARI dispersion within the RVOT was greater in BrS patients than controls (58±22ms vs 17±6ms; *p=0.04*). This was similar for ARIc dispersion. **Figure 5a** illustrates the prolongation and increase in ARI gradients within the RVOT in a BrS patient following ajmaline. We correlated the changes in RVOT dispersion with J point elevation but did not find a significant relationship using ARI (R=0.20, *p=0.50*) or ARIc (R=0.20, *p=0.52*) (**Figure 5b**). Similar results were observed when correlated with $ST_{40}$ and $ST_{80}$ elevation (**Table 3**).

**Discussion**

In this study, we describe the changes in conduction and action potential duration in non-spontaneous BrS human hearts in-vivo following ajmaline. Greater changes were observed in the RVOT than RV or LV re-affirming the site of the pathological substrate in this condition. Importantly, we demonstrated a correlation between J point elevation in the Type I BrS pattern and increasing conduction delay in the epicardial RVOT which further supports the depolarization hypothesis as the underlying electrophysiological mechanism of the Type I pattern seen.

***Differences in the RVOT, RV and LV in BrS***

Although the genetic abnormalities implicated in BrS affect individual ion channel functioning across the heart uniformly, the RVOT has been shown to be the site of the electrophysiological

substrate that gives rise to the BrS phenotype[12]. One explanation, likely lies in differences during embryonic development and ion channel expression between the RVOT, RV and LV[13]. Thus, it is of interest to determine the differential behaviour of the RVOT, RV and LV to sodium channel blockade, although few studies have examined the electrophysiological changes in these regions simultaneously in patients with non-spontaneous Type I pattern[2,3,14].

Body surface potential mapping data in BrS patients following ajmaline, has previously shown ~~a~~ significant increase in body surface filtered QRS duration in the precordial leads overlying the RV but not the LV[2]. Differences between the RV and RVOT were not commented upon owing to the methodological limitations in knowing the corresponding body surface potentials of the RV and RVOT. Another whole heart study employing ECGi in patients with a spontaneous Type I pattern showed that steeper repolarization gradients and higher mean activation durations were preferentially found in the RVOT compared to RV or LV within BrS subjects at resting baseline[5]. These studies, in addition to previous intracardiac electrophysiological mapping studies restricted to the RV/RVOT, support our findings that changes in conduction and repolarization following ajmaline predominantly affects the RVOT in comparison to RV or LV in the BrS heart[14-16].

***Changes in conduction and J-ST elevation***

Increase in ATD was most prominent in the RVOT and did not differ much between the RV and LV free wall (Figure 3) in the BrS patients. The embryonic RVOT differs in embryological origin to the LV and loses its slow conducting properties much later than the RV and LV during its development. It is purported that remnants of the embryonic outflow tract are present, as supported by findings of fibrosis and the presence of late potentials in the RVOT in a transplanted BrS heart[17]. Combined with genetic defects which alter the current available for

AP propagation (e.g. inward sodium ($I_{Na}$)), initiation of the AP in the RVOT occurs much later than the RV. The depolarization hypothesis considers that delayed activation in the RVOT, relative to the RV, creates an electrotonic gradient which gives rise to the ST elevation observed on the body surface electrodes over this region. It would thus follow that the magnitude of J-ST point elevation would correlate with the degree of activation delay in the RVOT, and not the RV or LV as confirmed in our results. Our findings are also similar to previous studies that have correlated filtered QRS duration from body surface mapping potentials and right ventricular conduction delay from echocardiography to ST elevation on the surface ECG[2,3]. Change in ATD observed in our study is relatively small and seemingly associated with large changes in J-ST elevation. It should be pointed out these measurements only reflect changes in conduction over a selected epicardial area, and may act as a surrogate for larger absolute changes in conduction that occur transmurally or across the entire myocardium[18].

***Changes in epicardial repolarization with J-ST point elevation***

In the repolarization hypothesis, transmural dispersion created by a more notched AP and longer APD from cells in the epicardium than endocardium is proposed to give rise to the ST elevation seen and is supported mainly by experimental data[1]. In one clinical study, ARIc from unipolar EGMs in the endocardial and epicardial RVOT were measured during electrophysiological catheter studies in nineteen BrS subjects[4]. Following sodium channel blockade with pilsicainide in nine individuals, Nagase et al reported a prolongation in ARIc in the epicardial RVOT but no change in the endocardium and reported this occurrence on manifestation with the BrS phenotype[4]. In contrast, other studies compared body surface

mapping potential and echocardiographic surrogates of repolarization with ST elevation following ajmaline and flecainide respectively, but found no correlation in either study[2,3].

Similar to Nagase et al, we have observed prolongation of ARI/ARIc in the epicardial RVOT occurring with the onset of the BrS phenotype. In addition, we demonstrate that ARIc prolongation occurs preferentially over this region compared to the RV and LV. However, we also show that changes in repolarization on the RVOT epicardium do not correlate with the degree of J point and ST elevation following sodium channel blockade. It should be pointed out that ECGi does not provide EGM data from the endocardium, and it is assumed that the changes to transmural dispersion following sodium channel blockade arise mainly from the ARIc prolongation in the RVOT epicardium, as previously shown by Nagase and colleagues.

Another surrogate of transmural dispersion of repolarization is the Tped[9]. Although a preferential increase in Tped occurred over the RV/RVOT region in BrS patients, there was no significant correlation with J point elevation. However, it has also been suggested that Tped from the surface ECG may reflect regional dispersion rather than transmural which limits the interpretation of our findings[19].

Prolongation of ARI/ARIc may also be related to the blocking effects of ajmaline on the transient potassium outward current ($I_{to}$)[20]. The greater prolongation in the whole RV (including RVOT) of ARI/ARIc than LV is in keeping with there being a smaller $I_{to}$ channel density in the LV (ARI: 25±25ms vs -2±19ms; *p<0.01*) (ARIc: 54±20ms vs 21±12ms; *p<0.01*)[13]. The differences between the RV and RVOT are less clear and may relate to a differential distribution density of $I_{to}$ channels in these regions. Interestingly, little change was observed within the RVOT and RV in the controls. Nagase and colleagues similarly observed no significant changes in ARIc in the RVOT in their three controls following pilsicainide. It is

possible that these differences in ARI prolongation observed between BrS and controls may relate to the amount of functioning $I_{to}$ channels available which would support the notion that non-SCN5a genetic mutations are also implicated in this syndrome[1].

Although we have not observed a correlation between J point or ST elevation with surrogates of transmural or transepicardial ARI dispersion, it may be premature to completely discount the repolarization hypothesis as a fundamental assumption has been made with ARI measurements. ARI derived from the unipolar EGM assumingly reflects a single AP duration as employed in several previous studies[4,5,12,14-16]. In a pharmacological wedge preparation model of BrS, Szel and Antzelevitch demonstrate that 'notching' within the ST segment observed in the unipolar EGM signal in BrS could relate to a second AP caused by concealed phase 2 re-entry. In these EGMs, the T wave is proposed to be related to the second depolarization[21] and ARI measurements may thus produce an erroneous result. In **Figure 3ai**, comparison has been made to the 'notching' observed in the coved ST segment of the unipolar ECGi EGM from the RVOT. Whilst we have no monophasic action potential data to determine if phase 2 re-entry is occurring in our patients, previous work has shown the presence of singular monophasic action potentials in the RVOT epicardium in BrS human studies[12,22]. We therefore assume the validity of using ARI to reflect APD as with other work in the literature[4,5,12,14-16].

***Limitations***

The number of controls in our study is small. However, the aim of this study was to correlate ST elevation and changes in depolarization and repolarization rather than to compare differences in BrS and normal hearts. Both our controls did not manifest the Type I pattern

despite receiving the full weight adjusted dosage of ajmaline, and provide important control points to this correlation study. It is also unclear what effects age, gender and individual genetic mutations have on this relationship between conduction delay and ST elevation. Evidence exists on the differences in ion channel distribution between the genders and age has an impact on conduction in SCN5a+ murine hearts[20,23]. The number of BrS cases in this study limits our ability to provide answers to these questions.

The RVOT studied is assumed to be the region encompassing the area four centimetres below the pulmonary valve as identified from the CT scan, and may have possibly included a small part of the RV at the junction of the outflow tract. The ATD examined within the heart only reflects specific areas within the RV and LV free wall. This was limited by being able to obtain the same measurement points along the activation wave fronts at baseline and following ajmaline. We believe that main regions of interest were studied and little additional information would be obtained by breaking the regions down further which are also fraught with other methodological difficulties.

Our study is also restricted to those with a concealed Type I BrS pattern and does not include any with a spontaneous Type I pattern for comparison. Although we are conducting a separate study in the latter group, an advantage of studying the concealed BrS group with ajmaline allows for each subject to serve as their own baseline control. Inter-individual variability in conduction and repolarization at baseline exists and would require a much larger number of patients with a spontaneous Type I pattern and varying ST elevation to derive any correlative data.

**Conclusion**

The strength of our study is in providing in-vivo epicardial whole heart and regional changes in conduction, repolarization and EGM morphology in response to ajmaline. More importantly, we demonstrate the underlying significance of the magnitude of ST elevation seen in the BrS pattern on the surface ECG. Our findings that conduction delay or excitation failure in the RVOT, and not prolongation of epicardial action potential duration, correlates with the BrS pattern provides further support for the depolarization hypothesis.

**Acknowledgements:** We are grateful to Mr Edward Cajalog for his assistance and support with the ajmaline test.

**Funding Sources:** KL was supported by a British Heart Foundation Project Grant (PG/15/20/31339) and The Dan Bagshaw Memorial Trust Fund. FSN was supported by an NIHR Clinical Lectureship (1716). CR was supported by the BHF Research Grant (RG/16/3/32175), NIHR (Clinical Lectureship LDN/007/255/A and BRC), and Imperial ElectroCardioMaths Programme.

**Disclosures:** PK has received honoraria from CardioInsight Inc.

**References**


1. Meregalli PG, Wilde AM, Tan HL. Pathophysiological mechanisms of Brugada syndrome: depolarization disorder, repolarization disorder, or more? *Cardiovasc Res*. 2005;67:367-378.
2. Postema PG, van Dessel PFHM, Kors JA Linnenbank AC, van Herpen G, van Eck JAK, van Geloven N, de Bakker JMT, Wilde AAM, Tan HL. Local Depolarization Abnormalities Are the Dominant Pathophysiologic Mechanism for Type 1 Electrocardiogram in Brugada Syndrome. A Study of Electrocardiograms, Vectorcardiograms, and Body Surface Potential Maps During Ajmaline Provocation. *J Am Coll Cardiol*. 2010;55:789-797.
3. Tukkie R, Sogaard P, Vleugels J, De Groot IKLM, Wilde AAM, Tan HL. Delay in Right Ventricular Activation Contributes to Brugada Syndrome. *Circulation*. 2004;109:1272-1277.
4. Nagase S, Kusano KF, Morita H, Nishii N, Banba K, Watanabe A, Hiramatsu S, Nakamura K, Sakuragi S, Ohe T. Longer repolarization in the epicardium at the right ventricular outflow tract causes type 1 electrocardiogram in patients with Brugada syndrome. *J Am Coll Cardiol*. 2008;51:1154-1161
5. Zhang J, Sacher F, Hoffmayer K, O'Hara T, Strom M, Cuculich P, Silva J, Cooper D, Faddis M, Hocini M, Haissaguerre M, Scheinman M, Rudy Y. Cardiac electrophysiological substrate underlying the ECG phenotype and electrogram abnormalities in Brugada syndrome patients. *Circulation*. 2015;131:1950-1959.
6. Vijayakumar R, Silva JN, Desouza KA, Abraham RL, Strom M, Sacher F, van Hare GF, Haissaguerre M, Roden DM, Rudy Y. Electrophysiologic Substrate in Congenital

Long QT Syndrome: Noninvasive Mapping with Electrocardiographic Imaging (ECGI). *Circulation*. 2014. 130:1936-1943.

7. Ramanathan C, Ghanem RN, Jia P, Ryu K, Rudy Y. Noninvasive electrocardiographic imaging for cardiac electrophysiology and arrhythmia. *Nat Med*. 2004;10:422-428.

8. Yue AM, Paisey JR, Robinson S, Betts TR, Roberts PR, Morgan JM. Determination of human ventricular repolarization by noncontact mapping: validation with monophasic action potential recordings. *Circulation*. 2004;110:1343-1350.

9. Yan G, Antzelevitch C. Cellular Basis for the Normal T Wave and the Electrocardiographic Manifestations of the Long-QT Syndrome. *Circulation*. 1998;98:1928-1936.

10. Wilde AAM, Antzelevitch C, Borggrefe M, Brugada J, Brugada R, Brugada P, Corrado D, Hauer RNW, Kass RS, Nademanee K, Prior SG, Towbin JA. Proposed Diagnostic Criteria for the Brugada Syndrome: Consensus Report *Circulation*. 2002;106:2514-2519.

11. Barnes AR, Katz LN, Levine SA, Pardee HEB, White PD, Wilson FN. Report of the committee of the American Heart Association on the standardization of electrocardiographic nomenclature. *Am Heart J* 1943;25:528-534

12. Nademanee K, Veerakul G, Chandanamattha P, Chaothawee L, Ariyachaipanich A, Jirasirirojanakorn K, Likittanasombat K, Bhuripanyo K, Ngarmukos T. Prevention of ventricular fibrillation episodes in Brugada syndrome by catheter ablation over the anterior right ventricular outflow tract epicardium. Circulation. 2011;123:1270–1279.

13. Boukens BJD, Christoffels VM, Coronel R, Moorman AFM. Developmental basis for electrophysiological heterogeneity in the ventricular and outflow tract

myocardium as a substrate for life-threatening ventricular arrhythmias. *Circ Res*. 2009;104:19-31.

14. Ten Sande JN, Coronel R, Conrath CE, Driessen AHG, De Groot JR, Tan HL, Nademanee K, Wilde AAM, de Bakker JMT, van Dessel PFHM. ST-Segment Elevation and Fractionated Electrograms in Brugada Syndrome Patients Arise from the Same Structurally Abnormal Subepicardial RVOT Area but Have a Different Mechanism. *Circ Arrhythmia Electrophysiol*. 2015;8:1382-1392.
15. Postema PG, van Dessel PFHM, de Bakker JMT, Dekker LRC, Linnenbank AC, Hoogendijk MG, Coronel R, Tijssen JGP, Wilde AAM, Tan HL. Slow and discontinuous conduction conspire in Brugada syndrome: a right ventricular mapping and stimulation study. *Circ Arrhythm Electrophysiol*. 2008;1:379-386.
16. Lambiase PD, Ahmed K, Ciaccio EJ, Brugada R, Lizotte E, Chaubey S, Ben-Simon R, Chow AW, Lowe MD, McKenna WJ. High-density substrate mapping in Brugada syndrome: combined role of conduction and repolarization heterogeneities in arrhythmogenesis. *Circulation*. 2009;120:106-117, 1-4.
17. Coronel R, Casini S, Koopmann TT, Wilms-Schopman FJ, Verkerk AO, de Groot JR, Bhuiyan Z, Bezzina CR, Veldkamp MW, Linnenbank AC, van der Wal AC, Tan HL, Brugada P, Wilde AA, de Bakker JM. Right ventricular fibrosis and conduction delay in a patient with clinical signs of Brugada syndrome: a combined electrophysiological, genetic, histopathologic, and computational study. Circulation. 2005;112:2769–2777.
18. Zhang P, Tung R, Zhang Z, Sheng X, Liu Q, Jiang R, Sun Y, Chen S, Yu L, Ye Y, Fu G, Shivkumar K, Jiang C. Characterization of the epicardial substrate for catheter ablation of Brugada Syndrome. Heart Rhythm 2016; 13:2151-2158.

19. Opthof T, Coronel R, Wilms-Schopman FJG, Plotnikov AN, Shlapakova IN, Danilo Jr P, Rosen MR, Janse MJ. Dispersion of repolarization in canine ventricle and the electrocardiographic T wave: Tp-e interval does not reflect transmural dispersion. *Heart Rhythm*. 2007;4:341-348.

20. Bébarová M, Matejovič P, Pásek M, Šimurdová M, Šimurda J. Effect of ajmaline on action potential and ionic currents in rat ventricular myocytes. *Gen Physiol Biophys*. 2005;24:311-325.

21. Szel T and Antzelevitch C. Abnormal repolarization as the basis for late potentials and fractionated electrograms recorded from the epicardium in experimental models of Brugada Syndrome. *J Am Coll Cardiol* 2014;63;2037-2045.

22. Eckardt L, Kirchhof P, Johna R, Breithardt G, Borggrefe M, Haverkamp W. Transient Local Changes in Right Ventricular Monophasic Action Potentials Due to Ajmaline in a Patient with Brugada Syndrome. J Cardiovasc Electrophysiol. 1999 ;10:1010-5.

23. Van Veen TAB, Stein M, Royer A, Quang KL, Charpentier F, Colledge WH, Huang CLH, Wilders R, Grace AA, Escande D, de Bakker JMT, van Rijen HVM. Impaired impulse propagation in Scn5a-knockout mice: Combined contribution of excitability, connexin expression, and tissue architecture in relation to aging. *Circulation*. 2005;112:1927-1935.

**Table 1 – Group characteristics. V1 and V2 are in the right and left 4th intercostal space (IC) respectively. IC2 – 2nd intercostal space. IC3 – 3rd intercostal space.**

| s/no | Gender | Age | Ajmaline Result | Maximal J point elevation (mm) | Type I pattern in Lead(s) | Previous SCD event | Time to positive ajmaline (mins) |
|---|---|---|---|---|---|---|---|
| 1 | M | 33 | + | 5 | $V2_{IC3}$ | - | 6 |
| 2 | M | 40 | + | 2.5 | $V1_{IC2}$ | - | 5 |
| 3 | M | 39 | + | 3 | $V1_{IC2}$; $V2_{IC3}$ | + | 6 |
| 4 | F | 69 | + | 2 | V1 | - | 6 |
| 5 | M | 32 | + | 2 | $V1_{IC2}$ | - | 5 |
| 6 | M | 50 | + | 4 | V2 | + | 6 |
| 7 | M | 52 | + | 4 | V2; $V2_{IC3}$ | + | 5 |
| 8 | F | 50 | + | 5 | V2 | - | 5 |
| 9 | F | 60 | + | 2.2 | V1 | - | 6 |
| 10 | M | 36 | + | 4 | $V2_{IC3}$ | - | 1.5 |
| 11 | F | 50 | + | 2 | V1 | - | 5 |
| 12 | M | 38 | - | 0 | V1 | - | n/a |
| 13 | F | 25 | - | 0.4 | V1 | - | n/a |

**Table 2 – Tpeak-end duration at baseline and following ajmaline**

| *Region* | *Leads* | *Brugada Syndrome* | | *Control* | | *Correlation of Tpe change to J elevation* | |
|---|---|---|---|---|---|---|---|
| | | **Baseline (ms)** | **Ajmaline (ms)** | **Baseline (ms)** | **Ajmaline (ms)** | **Pearsons R** | ***p value*** |
| *RV/ RVOT* | **V1 (IC2)** | **82±10** | **104±23** | **81±4** | **84±7** | **0.26** | **0.39** |
| | **V2 (IC2)** | **93±16** | **98±19** | **79±5** | **82±9** | **-0.24** | **0.43** |
| | **V1 (IC3)** | **83±13** | **107±25** | **74±7** | **79±5** | **0.37** | **0.22** |
| | **V2 (IC3)** | **90±17** | **110±26** | **86±23** | **91±21** | **0.32** | **0.29** |
| | **V1** | **85±16** | **109±18** | **60±11** | **65±9** | **0.57** | **0.06** |
| | **V2** | **96±16** | **112±13** | **95±1** | **95±3** | **-0.02** | **0.95** |
| | **Lead with max J elevation** | **85±15** | **106±20** | **60±11** | **61±12** | **0.44** | **0.13** |
| | | | | | | | |
| *LV* | **V4** | **95±11** | **95±14** | **75±5** | **77±7** | **-0.10** | **0.75** |
| | **V5** | **94±11** | **96±14** | **75±5** | **76±6** | **-0.01** | **0.99** |
| | **V6** | **89±12** | **87±11** | **77±7** | **77±7** | **0.06** | **0.85** |

**Table 3 – Correlation to $ST_{40}$ and $ST_{80}$ following ajmaline**

| ATD change | Correlation to $ST_{40}$ | *p value* | Correlation to $ST_{80}$ | *p value* |
|---|---|---|---|---|
| **RVOT** | 0.84 | 0.0003 | 0.91 | 0.0001 |
| **RV** | 0.27 | 0.37 | 0.25 | 0.41 |
| **LV** | 0.24 | 0.43 | 0.35 | 0.24 |
| | | | | |
| **ARI prolongation** | | | | |
| **RVOT** | 0.41 | 0.16 | 0.41 | 0.16 |
| **RV** | -0.79 | 0.78 | -0.11 | 0.73 |
| **LV** | 0.05 | 0.87 | 0.12 | 0.69 |
| | | | | |
| **Change in RVOT ARI dispersion** | 0.29 | 0.34 | 0.33 | 0.28 |
| | | | | |

**Figure Legends**

**Figure 1: (a)** ECGi system combining body surface potential data from a 252-electrode vest (i & ii) with CT derived heart-torso geometry (iii & iv) to produce epicardial unipolar electrograms and panoramic 3D electroanatomical maps (v). **(b)** The heart is anatomically divided into 15 segments with examples of unipolar electrograms in three regions shown. **(c)** Shows position of electrode of 15 lead ECG recording and measurement of J elevation and Tpeak to end duration.

**Figure 2**: **(a)** 3D activation maps of epicardial breakthrough during a sinus beat before and after ajmaline infusion, at maximal J point elevation, in a patient with BrS. Close up of the RVOT (red box) shows greater isochronal crowding, with corresponding delay in electrogram local activation timing at site 1, following ajmaline infusion. **(b)** Mean±SD changes in activation time duration in the RVOT, RV and LV are shown with the largest increase in the RVOT following ajmaline in BrS patients. ** $p<0.01$; *** $p<0.001$; ns – not significant.

**Figure 3**: **(a)** Changes in unipolar electrogram morphology in a BrS patient (i) and control (ii) following ajmaline. In the BrS patient, there is coving and T wave inversion following ajmaline in EGMs within the RVOT region but no change in EGM morphology in the RV or LV. ARI in the RVOT region are subsequent prolonged. In contrast, there is little change in morphology or ARI in the control patient despite the full ajmaline dose administered. **(b)** Mean ARI prolongation is greatest in the RVOT compared to the RV or LV in BrS patients. * $p<0.05$; ** $p<0.01$; ns – not significant.

**Figure 4**: **(a)** Correlation between maximal J point elevation following ajmaline and the corresponding changes in ATD in the RVOT at the same time point for all patients. **(b)** Correlation between maximal J point elevation following ajmaline and the corresponding ARIc prolongation in the RVOT at the same time point for all patients. **(c)** Correlation between

maximal J point elevation following ajmaline and the Tped changes in the RVOT/RV lead with maximal J elevation at the same time point for all patients.

**Figure 5: (a)** ARI map in the RVOT region of a BrS patient at baseline and following manifestation of the BrS pattern with ajmaline. One observes prolongation of ARI within the RVOT, and increase in maximal gradient or dispersion of ARI with ajmaline. **(b)** Maximal dispersion of ARI is correlated with J point elevation (and ST segment elevation – table 3)

**Figure 1**

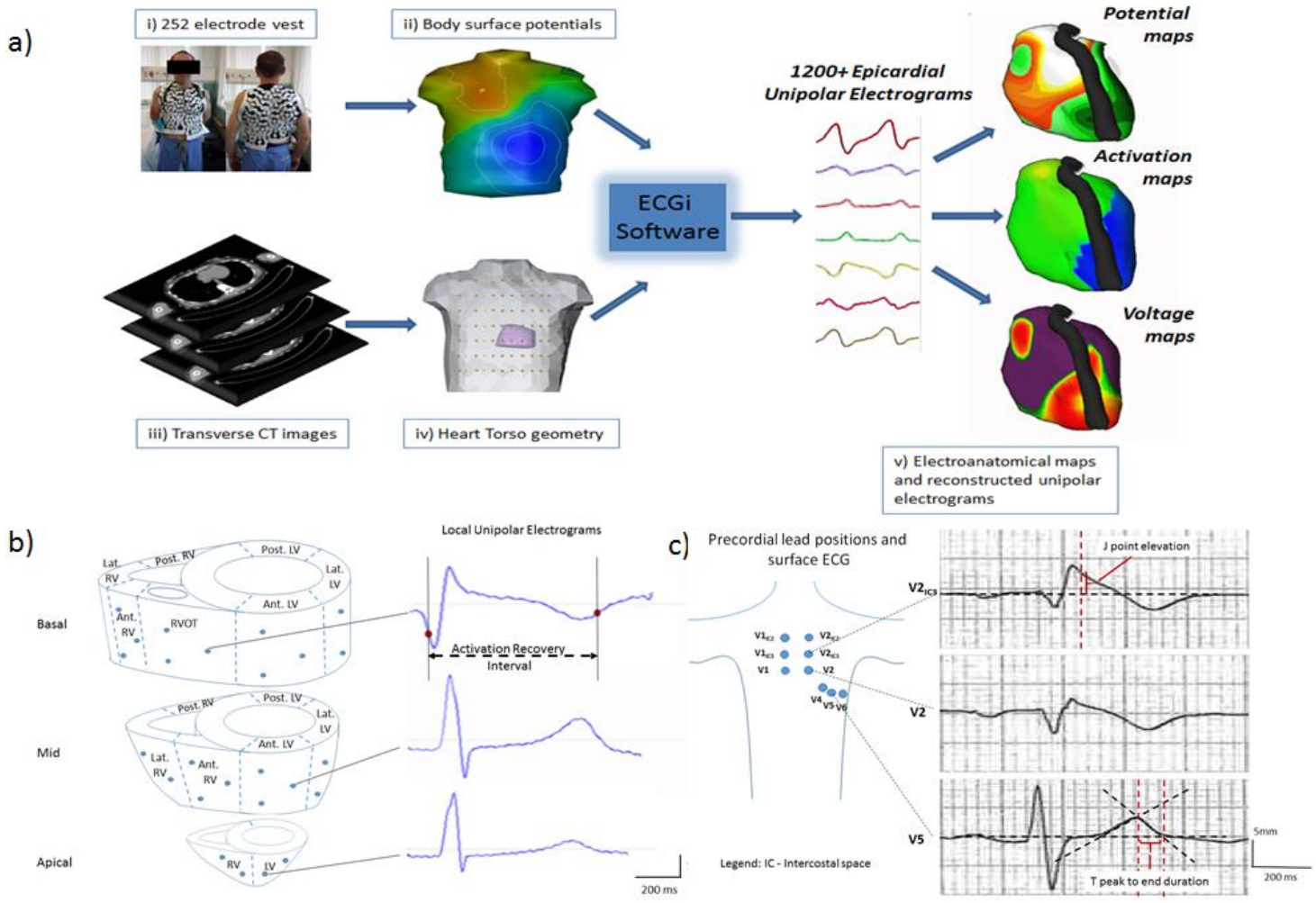


Key: LAD-left anterior descending artery; LV-left ventricle; RV-right ventricle; OT-outflow tract; ANT-anterior; POST-posterior; LAT-lateral

**Figure 2**

a)

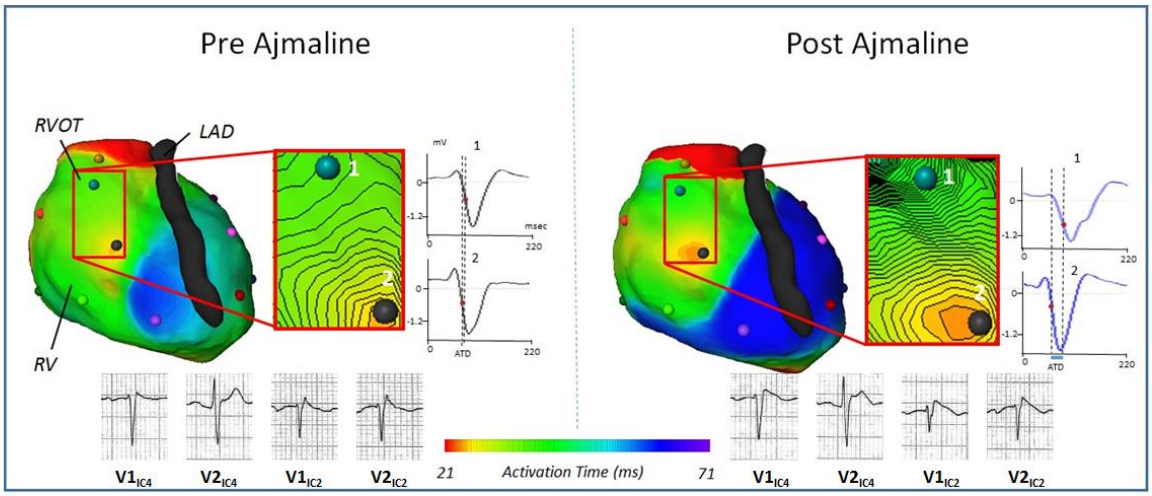
Pre Ajmaline
Post Ajmaline
RVOT
LAD
RV
mV
msec
ATD
220
1
2
V1IC4
V2IC4
V1IC2
V2IC2
21
Activation Time (ms)
71

b)

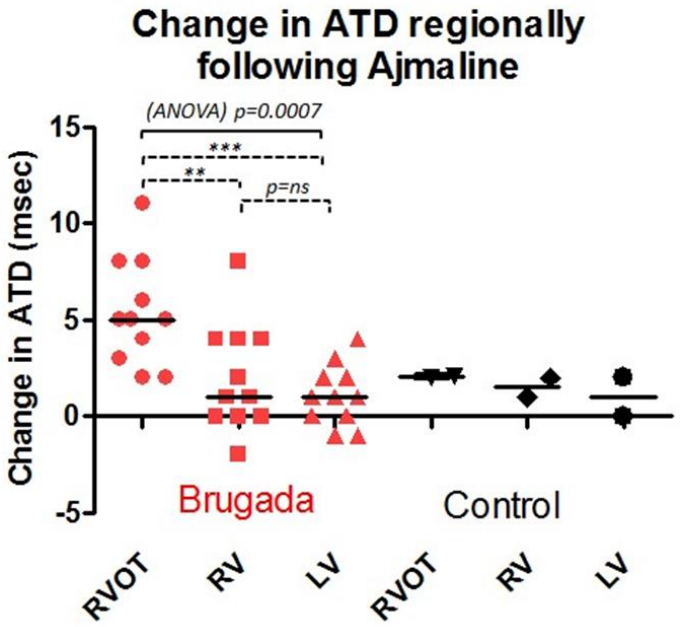
Change in ATD regionally following Ajmaline
(ANOVA) p=0.0007
***
**
p=ns
Change in ATD (msec)
15
10
5
0
-5
Brugada
Control
RVOT
RV
LV
RVOT
RV
LV

**Figure 3**

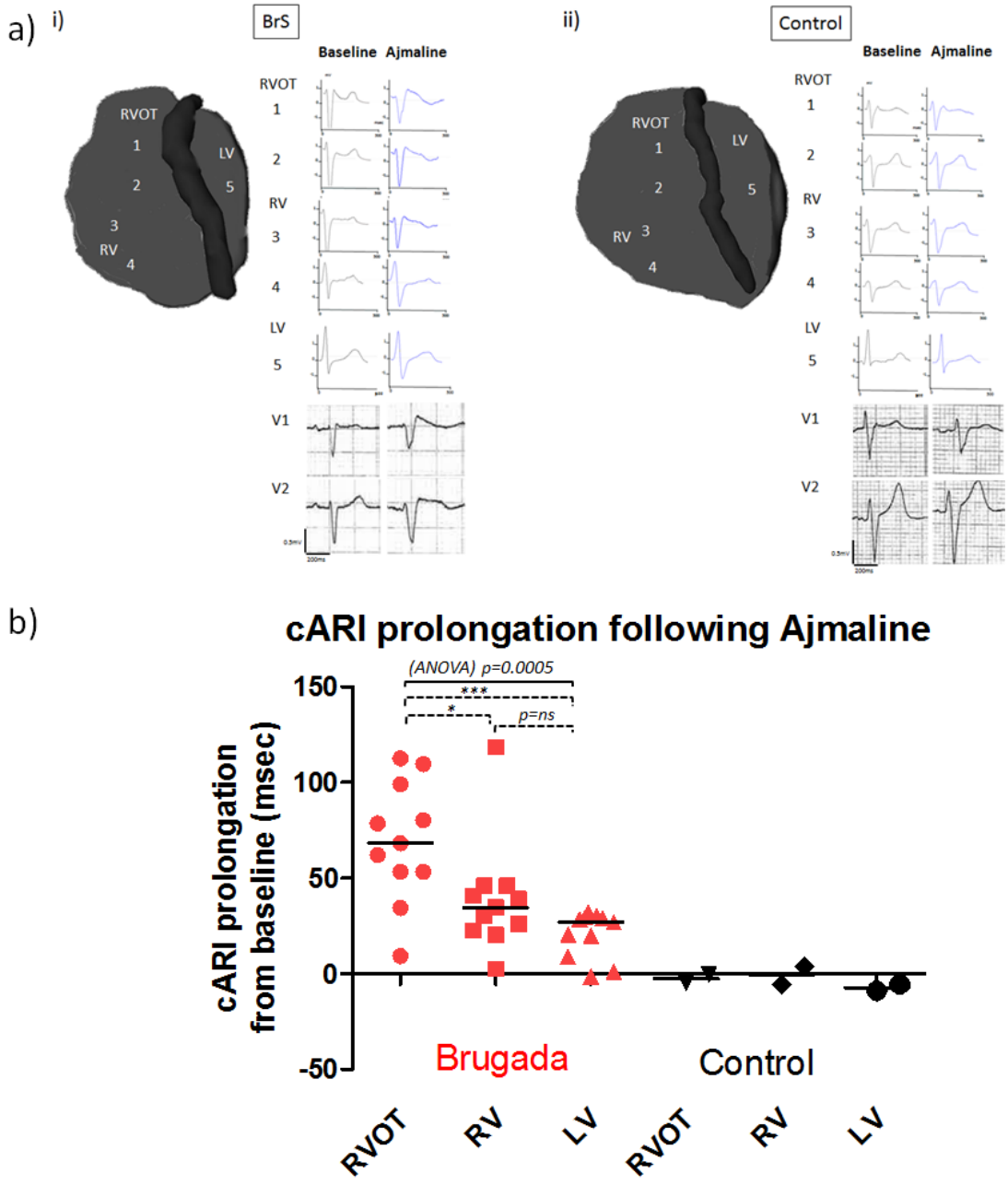
a)
i)
BrS
Baseline
Ajmaline
RVOT
1
2
RV
3
4
LV
5
V1
V2
ii)
Control
b)
cARI prolongation following Ajmaline
(ANOVA) p=0.0005
***
*
p=ns
cARI prolongation from baseline (msec)
150
100
50
0
-50
Brugada
Control
RVOT
RV
LV

**Figure 4**

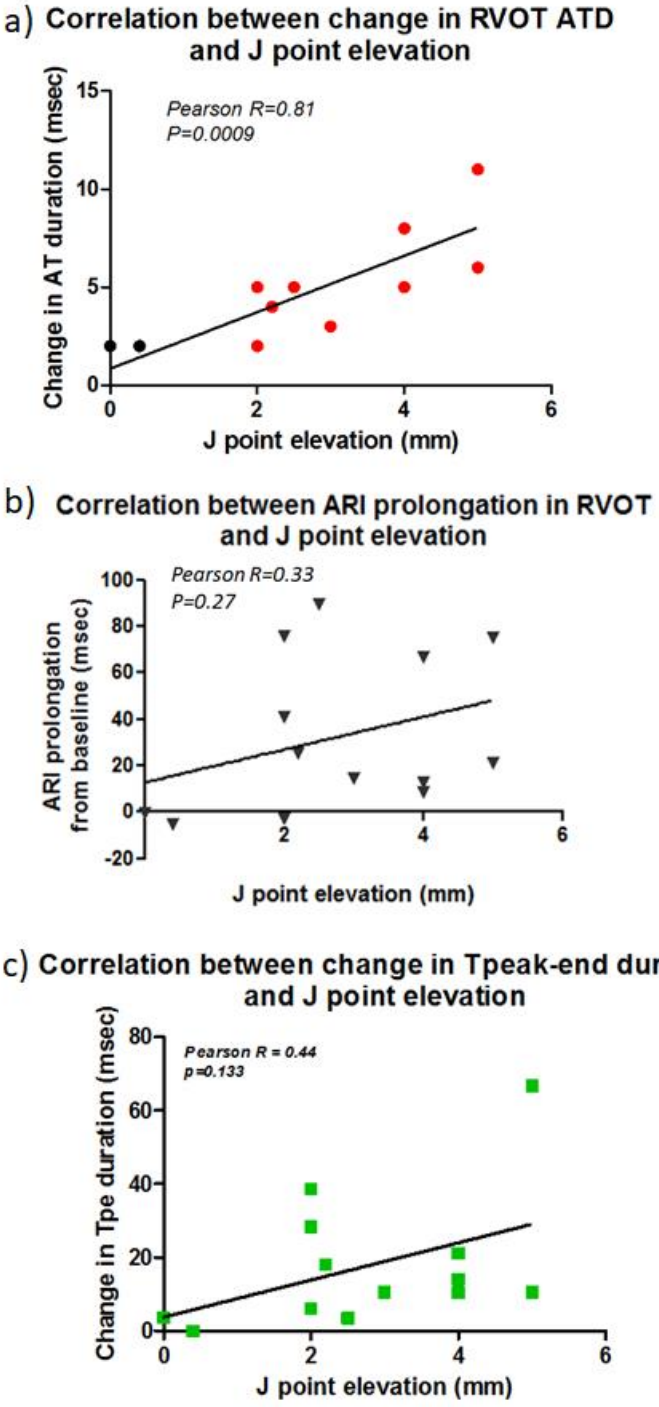
a) Correlation between change in RVOT ATD and J point elevation
Pearson R=0.81
P=0.0009
Change in AT duration (msec)
J point elevation (mm)
b) Correlation between ARI prolongation in RVOT and J point elevation
Pearson R=0.33
P=0.27
ARI prolongation from baseline (msec)
J point elevation (mm)
c) Correlation between change in Tpeak-end duration and J point elevation
Pearson R = 0.44
p=0.133
Change in Tpe duration (msec)
J point elevation (mm)

**Figure 5**

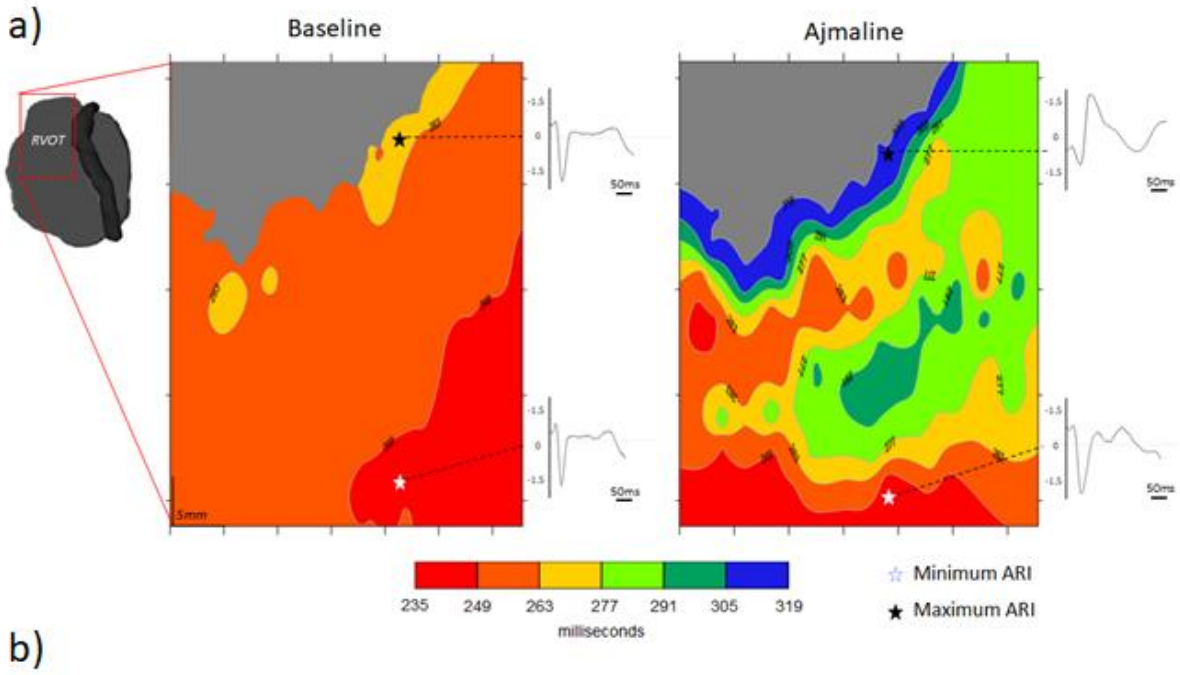
a)
Baseline
Ajmaline
RVOT
50ms
5mm
235
249
263
277
291
305
319
milliseconds
Minimum ARI
Maximum ARI

b)

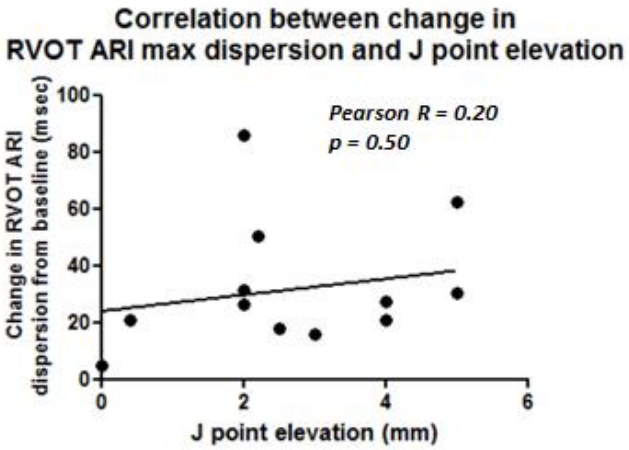
Correlation between change in
RVOT ARI max dispersion and J point elevation
Pearson R = 0.20
p = 0.50
Change in RVOT ARI
dispersion from baseline (msec)
J point elevation (mm)
0
20
40
60
80
100
0
2
4
6